Nat. Hazards Earth Syst. Sci. Discuss., https://doi.org/10.5194/nhess-2018-357
Manuscript under review for journal Nat. Hazards Earth Syst. Sci.
Discussion started: 14 December 2018

Natural Hazards and Earth System Sciences
Discussions

The effect of increased resolution of geostationary satellite imageries on predictability of tropical thunderstorms over Southeast Asia

Kwonmin Lee[1], Hye-Sil Kim[2] and Yong-Sang Choi[1]*

[1]Department of Climate and Energy Systems Engineering, Ewha Womans University, Seoul, South Korea
[2]Department of Atmospheric Science and Engineering, Ewha Womans University, Seoul, South Korea

Correspondence to: Prof. Yong-Sang Choi (ysc@ewha.ac.kr)

Abstract.

Tropical thunderstorms cause heavy damage to property and lives, and there is a strong interest in advancing the predictability of thunderstorms with more precise satellite observations. Using high-resolution (2 km and 10 minutes) imageries from the geostationary satellite (Himawari-8) recently launched over Southeast Asia, we examine how early the thunderstorms can be predicted compared to the low-resolution (4 km and 30 minutes) imageries of the former satellite. We compare the lead times for eight thunderstorms that occurred in August 2017 between high- and low-resolution imageries. These thunderstorms are identified by pixels with a brightness temperature at 10.45 μm (BT11) gradually decreasing by more than 5 K per 10 minutes (15 K per 30 minutes) compared to the previous imagery. The lead time is then calculated as the time passed from the initial to the mature stage of the thunderstorm signal, based on the time series of a minimum BT11 of these pixels. The lead time is found to be 100-180 minutes for the high-resolution imagery, while it is only found to be 30 minutes if detectable at all for the low-resolution imagery. This result suggests that the high-resolution imagery is essential for substantial disaster mitigation because of its ability to note an alarm more than two hours ahead of a matured thunderstorm.

1 Introduction

Climate change adaptation and disaster risk management integration are increasingly important issues since unpredictable natural hazards have appeared more frequently and intensively in the recent warmer climate (Shaw et al., 2010). Southeast Asia is the most vulnerable region of all due to the combination of climate-related hazards it faces, such as tropical cyclones, floods, droughts, and rises in sea level (Yusuf and Francisco, 2009). These severe events lead to extensive economic lost, environmental degradation, and subsequently, damage to human life.

Nat. Hazards Earth Syst. Sci. Discuss., https://doi.org/10.5194/nhess-2018-357
Manuscript under review for journal Nat. Hazards Earth Syst. Sci.
Discussion started: 14 December 2018

Natural Hazards and Earth System Sciences Discussions

In order to reduce hazardous risk, accurate weather forecasts are crucial. An extreme weather event can involve multiple hazards either simultaneously or in quick succession. For example, in addition to high winds and heavy rain, a tropical storm can result in flooding and mudslides (Nastos and Dalezios, 2016). Therefore, it is important to know how quickly early clouds can be detected before maturity in order to reduce disaster damage, because early clouds have a high possibility of being accompanied by heavy rain or lightning in the mature state (Houze, 1981). However, it is challenging to predict a convective system, because numerical weather prediction models generally have coarser spatiotemporal resolutions than deep convective clouds area with short life spans (Avotniece et al., 2017). Not only is the model itself insufficient, but the observational data are also insufficient in Southeast Asia. In this case, unlike mid-latitudes, tropical atmospheres are conditionally unstable and unpredictable. Therefore, alarms for those kinds of hazards are generally managed by the nowcast system by real-time observations, i.e., radar measurements on the ground and meteorological satellites. This means that advances in observation techniques should be grounded in order to improve pre-disaster risk management.

The observations of geostationary satellites have been particularly emphasized for convective clouds, considering their extensive spatial coverage (Escrig et al., 2013). Satellites can observe clouds regardless of them being over land or ocean, and they can also monitor the spans of clouds along their tracks (de Coning et al., 2015). Furthermore, geostationary satellite imagers have been greatly advanced in recent years. For example, high-resolution interval imagery of 2 km resolution and 10 minutes (briefly, min) by the Himawari-8 satellite operated by the Japan Meteorological Agency has been primarily available from the geostationary orbit since 2015 (Bessho et al., 2016). Similar resolution imageries can be obtained by several geostationary satellites: Geostationary Operational Environmental Satellites (GOES) (Menzel and Purdom, 1994), Fengyun-4 (FY-4) (Yang et al., 2017), and GEO-KOMPSAT-2A (GK2A) (Choi and Ho, 2015). These high-resolution observations have high potential to improve thunderstorm monitoring. Moreover, these satellites are not susceptible to hazards, and continuously provide enhanced thunderstorm information, unlike ground measurements.

As the number of recent meteorological geostationary satellites loading the enhanced imager increases, people expect to receive higher quality weather information than was available in the past. However, there has been a lack of prior attempts to quantify the predictability of thunderstorms using geostationary infrared imagers. In particular, using the improved imagery, we wonder how much earlier thunderstorms can be predicted than they could be using the prior imagery. In an attempt to resolve this shortcoming, this study focuses on tropical thunderstorm predictability based on spatiotemporal resolutions of imagery. We will demonstrate how much the predictability of initial thunderstorms can be improved using the Himawari-8 satellite.

2 Data and Method

The region of interest of this study is 5°-20°N and 100°-110°E, which is closely related to the Mekong River Commission. The Mekong River Commission is the only inter-governmental organization that works directly with the governments of

Cambodia, Lao PDR, Thailand, and Viet Nam to jointly manage the shared water resources and the sustainable development of the Mekong River (Jacobs, 2002).

Unfortunately, this is known as a vulnerable-disaster region because of a high risk of extreme weather. Disasters after hazards are distinctly common during the wet season, which generally starts around May and extends until October in Southeast Asia. In order to be suitable for our research purposes, we will focus on thunderstorms growing during the daylight hours in August. Table 1 shows eight selected convective clouds which are dramatically uprising in the clean sky, excluding clouds for which the development of the cloud was not visible on the surface due to the influence of the monsoon.

Himawari-8 is one of the recently-launched geostationary meteorological satellites and the first one capable of observing Southeast Asia. Himawari-8/9 has 16 observation bands, 11 more than the previous satellite, MTSAT-1R/2, as shown in Table 2. Simply, the spatial resolution is doubled and the time interval is tripled compared to the former. Himawari-8 can scan five areas and each area has a different time cycle. In the table, the Japan area (Regions 1 and 2) and the target area (Region 3) can be observed every 2.5 min and the landmark area can be observed every 0.5 min. However, depending on the region of interest of this study, convective cloud observations are possible every 10 minutes based on the full disk (JMA/MSC: Himawari-8/9 Imager (AHI), 2017).

In order to carry out this study, we make virtual data whose resolution is same as the MTSAT explained in Table 2. Specifically, four pixels of 2 km were converted into one pixel of 4 km, and the time interval was increased from 10 min to 30 min, which is the same as the former spatial resolution and time cycle. Hereafter, the virtual MTSAT will be called the 4 km and 30 min imager and the Himawari-8 will be called the 2 km and 10 min imager so as to help intuitive understanding of spatiotemporal resolution difference. Ultimately, showing the advanced predictability of deep convective clouds quantitatively of 2 km and 10 min imager compared to the 4 km and 30 min imager is our study goal.

Among 16 bands, one infrared band at 10.45 μm is used for monitoring the vertical growth of clouds. Measurements at 10.45 μm are less sensitive to ozone or water vapor in the atmosphere than any other infrared window bands (Schmit et al., 205). Thus, the brightness temperature at 10.45-μm for cumulus/convective clouds is closely related to the cloud top temperature. The colder cloud top and larger cloud thickness as the clouds develop vertically will effectively reduce the radiance and BT11. In particular, this study only uses the infrared band at 10.45 μm, which is the channel common to both Himawari-8 and MTSAT-1R, and the brightness temperature at 10.45 μm is rounded up to the decimal place and converted to an integer value as BT11.

3 Determining thunderstorm pixels and defining the lead time

Temporal changes in BT11 are deterministic variables that inform vertical drift velocity, the current statuses of clouds, and diagnose the probability of imminent heavy rains/lightning soon. We considered the monitoring ability of changes in minimum BT11 of clouds, which insofar, has been shown to be highly associated with the predictability of thunderstorms. In order to reflect the characteristics of suddenly developing thunderstorms, pixels with BT11 values gradually decreasing by

more than 5 K within 10 min (15 K in 30 min) compared to the previous one are selected. These pixels are then regarded as the thunderstorm pixels, and the smallest among them represents the cloud top temperature near the center of the convective cloud.

In order to determine the lead time, we should determine when the clouds start and when they become mature. As shown in Figure 1, the initial point is defined as the moment when the thunderstorm pixels are first detected, and the mature point means the change point where the minimum BT11 decreases gradually below 230 K and then increases again within the observation. Here, the definition of lead time is the time passed from when the cloud was initially detected to the mature point. The minimum BT11 at 230 K can be used as a parameter of the mature point, because when the minimum BT11 is near 230 K, the maximum of ice effective radius occurs (Kahn et al., 2018). The cloud drop size has an impact on the growth rate. For example, even though about 75 % of the droplets are less than 10 μm in the cloud, droplets > 10 μm made a major contribution to the growth (Wang, 2013). Additionally, the importance of the large ice effective radius of the cloud is closely related to rain formation. That is, the decline of minimum BT11 to 230 K or less means that the cloud grows vertically, while the increase of BT11 after reaching the mature point means that the cloud is enlarged as the horizontal movement becomes more dominant than the vertical motion. In particular, the precipitation occurring in a region where the mature cloud is within 50 km is called convective precipitation and that is where the heavy rain is usually concentrated (Houze, 204). In other words, we focus on clouds whose sizes are less than 50 km at the mature point.

Meanwhile, when the observation time is between 4:20 UTC and 5:40 UTC, the minimum value of BT11 slightly increases. This happening is commonly observed in the tropics when small clouds are gathering and overlapping before growing into a dominant convective system. In fact, small tropical convective clouds grow through various mechanisms as they overlap or split out. Thus, many meteorologists are likely to face this confusion in the cloud development process when attempting to predict thunderstorms. If the observation time interval is narrow, it is helpful to understand or track detailed changes in the cloud. That is why the more precise resolution is required for observing clouds at tight time intervals. In this study, we focus on the lead time and ignore the specific trend of BT11 between the first point and the maturing point.

4 Improved predictability by comparing lead time difference

The detection of cloud initiation is essential for the mitigation of hazards. The sooner early clouds can be detected in the cumulus stage, the better it is for more people to be alerted ahead of time for prompt evacuation. Some previous studies have shown the scale of a mesoscale convective system causing precipitation; the convective region covers from 30 km to 50 km and consists of intense rain, while the strati-form region covers from 100 km to 120 km and produces light rain. We focused on the convection region that causes heavy rainfall, and selected eight clouds with a cloud size of less than 50 km at the mature point, as shown in Table 3. Of the total of eight clouds, three occurred on August 10, 2017, and five occurred on August 11, 2017. August is one of the months with the most frequent occurrences of tropical thunderstorms in Southeast Asia during the rainy season. Among them, we chose the 10th and 11th days without being affected by the typhoon or

monsoon. Specifically, it was analyzed during the early stages of thunderstorms, which were not detected before daytime (3:00 - 5:50 UTC). The main reason we focused on daytime is that the floating population is most active during the daytime, which can be effective in reducing physical and human loss by predicting thunderstorms in the Mekong region. In total, eight clouds are selected in this paper, but the specific locations of these clouds are different.

As a result, in the cases of the 2 km and 10 min imager, the lead time is from 180 min to 100 min. In contrast, the 4 km and 30 min imager only began to detect cloud pixels up to 30 min before. Of the eight clouds, two made the 30 min prediction, and six clouds had zero lead time. (Here, a zero lead time means that the 4 km and 30 min imager failed to detect the cloud pixel when the cloud observed at 2 km and 10 min imager reached the mature point.) In summary, the latter satellite results in a four-fold improvement in lead time compared to the former. Thus, the higher the resolution, the more precisely the change rate of minimum BT11 is per pixel. For example, only one cloud pixel can be reflected on the area of 16 km2 in the case of the 4 km resolution imagery; in contrast, four cloud pixels can be reflected on the same area in the case of the 2 km and 10 min imager. In particular, we could not ignore either the influence of the resolution on the boundary of the cloud or the initial stage of cloud growth, when temperature change is rapid. As the time interval gets shorter, it is possible to observe the movement of the cloud in real time, and this helps the accurate prediction as well as the accumulation of data. In particular, the 4 km and 30 min imager cannot detect initial clouds whose scale is between 2 km and 4 km, so it is difficult to track the whole development process of thunderstorms. Therefore, the prediction of initial clouds through Himawari-8 shows the possibility of detection about two hours earlier than the MTSAT-1R.

Normally, a rapidly developing storm grows vertically at an early stage as quickly as it develops within 1-2 hours. According to the result, it is difficult to reflect the whole cloud with the 4 km and 30 min imager because the lead time is less than 30 min. In order to see if we can track the development of the cloud with the 2 km and 10 min imager during the lead time, we used BT11 observations images and timeline of the number of cloud pixels. Figure 2 shows the development process of the cloud on August 10, 2017, which is the same case shown in Figure 1. Figure 2a includes the development process of the cloud through BT11 images at 3:30, 4:20, 5:00, and 5:40 UTC. Figure 2b demonstrates the timeline of the number of cloud pixels during lead time. The gray boxes in Figure 2b mean the same time as the BT 11 images shown in Figure 2a. The first detection of cloud pixels occurs at 3:30 UTC, and several small clouds can be seen in Figure 2a. Then, several clouds are growing with the increase of cloud pixels in Figure 2b. However, as the clouds begin to overlap one another at 4:20 UTC, one dominant cloud is created at 5:00 UTC. Similarly, the number of cloud pixels changes from increasing to decreasing at 4:20 UTC in Figure 2b. One dominant cloud continuously develops and the area of the cloud expands from 5:00 to 5:40 UTC in Figure 2a. Finally, at 5:40 UTC, the number of cloud pixels reaches the highest value in Figure 2b. Therefore, the 2 km and 10 min imager is advantageous for tracking the entire developmental process during the lead time.

Nat. Hazards Earth Syst. Sci. Discuss., https://doi.org/10.5194/nhess-2018-357
Manuscript under review for journal Nat. Hazards Earth Syst. Sci.
Discussion started: 14 December 2018

5 Conclusion and limitation

This study shows that higher spatial and temporal resolutions of satellite observations are more effective for warning people of severe weather from convective clouds over Southeast Asia. In order to clarify the apparent impact of improved resolutions on monitoring clouds, we compared one infrared channel at 10.45 μm imagery of the 2 km and 10 min imager with that of the 4 km and 30 min imager. In the case of forecasting deep convective clouds by the infrared imagery with 4 km and 30 min imager over Southeast Asia, satellite observations are limited to capturing rapid changes in updraft in clouds. In contrast, imagery with the 2 km and 10 min imager can capture clouds 100-180 minutes before the cloud matures and begins falling as precipitation.

In order to more accurately examine the length of time between the initially detected cumulus and the mature deep convective with heavy rain, validation with precipitation data based on ground observation is further required. Thus, it is premature to assure the lead time for forecasting deep convective clouds over Southeast Asia by this study.In addition, the lead time can differ depending on the region, since the lead time can be affected by various environmental factors such as wind direction and speed, atmospheric profiles, and the characteristics of the geolocation. However, the point that we addressed here is that improved spatial and temporal resolutions of satellites clearly give benefits for enhancing the accuracy of the now-casting forecast.

What is not discussed in this study is the impact of increased spectral observations. The additional channels in Himawari-8 are another issue that improve the accuracy in forecasting deep convective clouds, compared to the former satellites. For example, three water vapor channels with different weighting functions can provide more detailed information about the vertical growth of cloud objects. The CO2 absorption channel also gives a chance to monitor temporal changes in cloud thickness and height. Another infrared channel, 8.6 μm, helps examine changes in glaciation in clouds. Therefore, utilizing new additional channels in Himawari-8 plays a role in reducing the false alarm rate related to thunderstorm prediction. We will examine the impact of additional multiple channels to monitoring deep convective clouds for the future study.

If applied to real technology, many developing countries in Southeast Asia may use the Himawari-8 satellite data for thunderstorm alarms. These countries include Bangladesh, Cambodia, Federated States of Micronesia, Myanmar, Palau, Papua New Guinea, Thailand, Tuvalu, and Viet Nam. However, few countries carefully consider satellite resolutions prior to applying satellite data for their forecast services to manage natural disasters. For example, Cambodia has been receiving Himawari-8 observations in recent years, but the spatial resolutions of their received satellite data are 4 km. In terms of expenditure for data storage, 4 km resolution data is more beneficial than 2 km resolution. However, as shown in this study, the 4 km resolution data is very limited for predicting thunderstorms. We suggest that the 2 km resolution data need to be disseminated to developing countries of Southeast Asia if possible. In 2018, another geostationary satellite similar to Himawari-8 will be launched in South Korea. It is expected that the study of thunderstorm prediction using high-resolution geostationary satellites will become more active in the future. Moreover, it will be an excellent tool for preparation and mitigation of hazards.

6 Summary

Thunderstorm prediction using satellites is of vital importance in Southeast Asian developing countries to reduce risks from heavy rain, lightning, and flooding. While recent satellites can observe the area more precisely and their applications to pre-disaster management are highly demanded, how far ahead the predictions of thunderstorms can be advanced was questionable. Our results show that thunderstorms can be predicted 100-180 minutes ahead of their matured stages, using the latest geostationary satellite data (2 km and 10 min resolutions). These data can readily capture rapidly-growing cloud tops before the clouds fall as precipitation. However, thunderstorms cannot be detected, or can only be detected 30 minutes ahead of time with the low-precision satellite data (4 km and 30 min resolutions). Notably, South Asian developing countries are currently receiving these low-precision satellite data.

Acknowledgements

This research was supported by Basic Science Research Program through the National Research Foundation of Korea (NRF) funded by the Ministry of Education (2018R1A6A1A08025520).

References

Avotniece, Z., Aniskevich, S., Briede, A., and Klavins, M.: Long-term changes in the frequency and intensity of thunderstorms in Latvia, BOREAL ENVIRONMENT RESEARCH., 22, 415-430, https://doi.org/10.2166/nh.2008.033, 2017.

Bessho, K., Date, K., Hayashi, M., Ikeda, A., Imai, T., Inoue, H. . . . and Okuyama, A.: An introduction to Himawari-8/9—Japan's new-generation geostationary meteorological satellites, Journal of the Meteorological Society of Japan., Ser. II, 94(2), 151-183, https://doi.org/10.2151/jmsj.2016-009, 2016.

Choi, Y. S. and Ho, C. H.: Earth and environmental remote sensing community in South Korea: A review, Remote Sensing Applications: Society and Environment, 2, 66-76, https://doi.org/10.1016/j.rsase.2015.11.003, 2015.

de Coning, E., Gijben, M., Maseko, B. and van Hemert, L.: Using satellite data to identify and track intense thunderstorms in South and southern Africa, South African Journal of Science, 111(7-8), 1-5, https://doi.org/10.17159/sajs.2015/20140402, 2015.

Escrig, H., Batlles, F. J., Alonso, J., Baena, F. M., Bosch, J. L., Salbidegoitia, I. B., & Burgaleta, J. I.: Cloud detection, classification and motion estimation using geostationary satellite imagery for cloud cover forecast, Energy, 55, 853-859, https://doi.org/10.1016/j.energy.2013.01.054, 2013.

Houze Jr, R. A., and Betts, A. K.: Convection in GATE, Reviews of Geophysics, 19(4), 541-576, https://doi.org/10.1029/rg019i004p00541, 1981.

Houze Jr, R. A.: Mesoscale convective systems, Reviews of Geophysics, 42(4), https://doi.org/10.1029/2004rg000150, 2004.

Jacobs, J. W.: The Mekong River Commission: transboundary water resources planning and regional security, Geographical Journal, 168(4), 354-364, https://doi.org/10.1111/j.0016-7398.2002.00061.x, 2002.

Himawari-8/9 Imager (AHI): https://www.data.jma.go.jp/mscweb/en/himawari89/space_segment/spsg_ahi.html, last access: 26 October 2018.

Kahn, B. H., Takahashi, H., Stephens, G. L., Yue, Q., Delanoë, J., Manipon, G. ... and Heymsfield, A. J.: Ice cloud microphysical trends observed by the Atmospheric Infrared Sounder, Atmospheric Chemistry and Physics, 18(14), 10715-10739, https://doi.org/10.5194/acp-18-10715-2018, 2018.

Menzel, W. P. and Purdom, J. F.: Introducing GOES-I: The first of a new generation of geostationary operational environmental satellites, Bulletin of the American Meteorological Society, 75(5), 757-782, https://doi.org/10.1175/1520-0477(1994)075<0757:igitfo>2.0.co;2, 1994.

Nastos, P., Dalezios, N. R. and Ulbrich, U.: Advances in meteorological hazards and extreme events, Special Issue of NHESS, https://doi.org/10.5194/nhess-16-1259-2016, 2016.

Schmit, T. J., Gunshor, M. M., Menzel, W. P., Gurka, J. J., Li, J. and Bachmeier, A. S.: Introducing the next-generation Advanced Baseline Imager on GOES-R, Bulletin of the American Meteorological Society, 86(8), 1079-1096, https://doi.org/10.1175/bams-86-8-1079, 2005.

Shaw, R., Pulhin, J. and Pereira, J.: Climate change adaptation and disaster risk reduction: an Asian perspective. Bingley, https://doi.org/10.1108/s2040-7262(2010)0000005007, 2010.

Wang, P. K.: Physics and dynamics of clouds and precipitation, Cambridge University Press, 2013.

Yang, J., Zhang, Z., Wei, C., Lu, F. and Guo, Q.: Introducing the new generation of Chinese geostationary weather satellites, Fengyun-4, Bulletin of the American Meteorological Society, 98(8), 1637-1658, https://doi.org/10.1175/bams-d-16-0065.1, 2017.

Yusuf, A. A. and Francisco, H.: Climate change vulnerability mapping for Southeast Asia, 2009.

Nat. Hazards Earth Syst. Sci. Discuss., https://doi.org/10.5194/nhess-2018-357
Manuscript under review for journal Nat. Hazards Earth Syst. Sci.
Discussion started: 14 December 2018

Natural Hazards and Earth System Sciences Discussions

Tables

Table 1. The observation time and number of observed clouds in this study.

Date	Observation time	Number of observed clouds
August 10, 2017	3:00-5:50 UTC	3
August 11, 2017	3:00-6:50 UTC	5

Table 2. Advanced Himawari Imager (AHI) information compared with MTSAT; the spatial resolution is doubled and the time interval is tripled compared to the former.

	Himawari-8/9		MTSAT-1R/2	
Spatial resolution	Band 3	0.5 km	Band 3	1 km
	Band 1,2,4	1 km	-	-
	Band 5-16	2 km	Band 7,8,13,15	4 km
Time interval	Full Disk	10 min	Full Disk	30 min
	Japan Area and Target Area	2.5 min		
	Landmark Area	0.5 min		

Table 3. Comparison of lead time according to imager (asterisk (*) denotes the case shown in the figures).

No.	Date	Cloud scale	Lead time (min)		Lead time difference
			2 km and 10 min imager	4 km and 30 min imager	
1	August 10, 2017	20 km	110	0	110
2*		20 km	140	0	140
3		24 km	120	0	120
4	August 11, 2017	28 km	100	0	100
5		40 km	180	30	160
6		28 km	180	0	180
7		16 km	160	0	160
8		36 km	180	30	160

Nat. Hazards Earth Syst. Sci. Discuss., https://doi.org/10.5194/nhess-2018-357
Manuscript under review for journal Nat. Hazards Earth Syst. Sci.
Discussion started: 14 December 2018

Natural Hazards and Earth System Sciences
Discussions

Figures

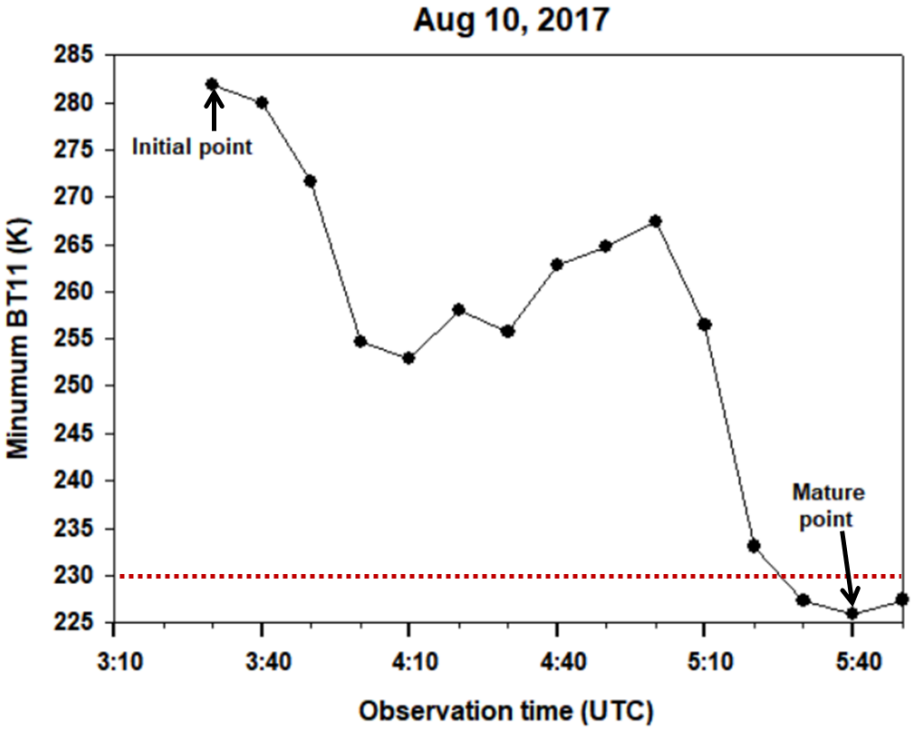

Figure 1. A trend of BT11 during observation time (August 10, 2017); The initial point is the moment when the thunderstorm pixel is first detected and the mature point is the change point where the minimum BT11 decreases gradually below 230 K (red line in Figure 1), and then increases again. In addition, the definition of lead time is the time when the initial point started from the mature point.

Nat. Hazards Earth Syst. Sci. Discuss., https://doi.org/10.5194/nhess-2018-357
Manuscript under review for journal Nat. Hazards Earth Syst. Sci.
Discussion started: 14 December 2018

Natural Hazards and Earth System Sciences
Discussions

a

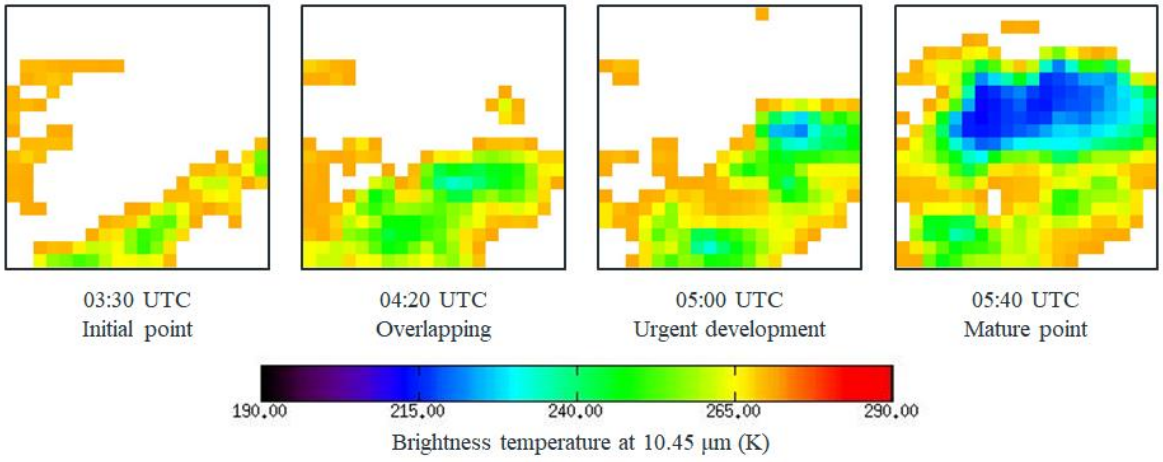

b

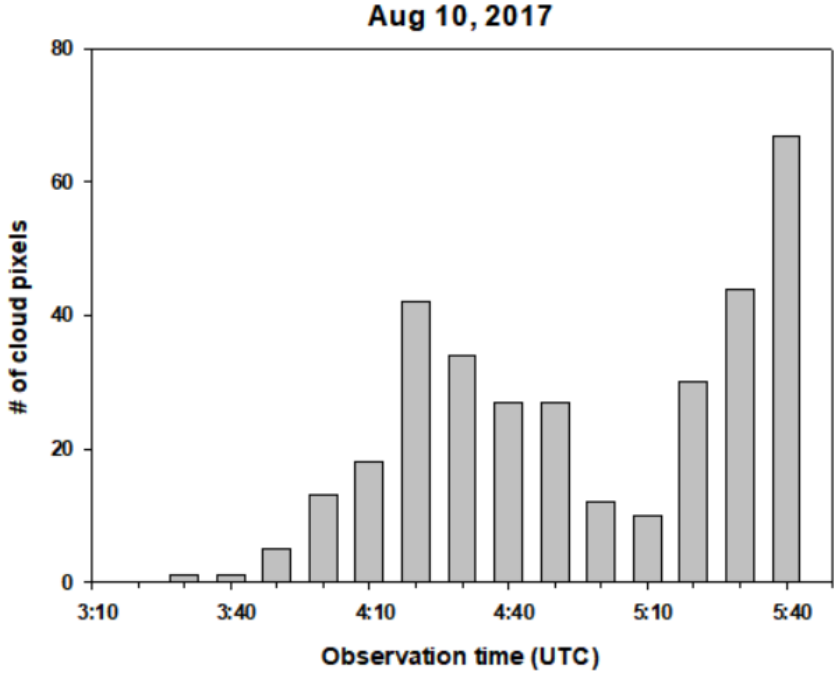

Figure 2. (a) The development process of cloud through BT11 images at 3:30, 4:20, 5:00, and 5:40 UTC, (b) Timeline of the number of detected cloud pixels during lead time; Cloud pixels are first detected at 3:30 UTC and several small clouds are overlapping at 4:20 UTC. Then, the single dominant cloud begins to develop rapidly at 5:00 UTC and finally reaches the mature point at 5:40 UTC.